Permeability estimation from the joint use of stoneley wave velocity and support vector machine neural networks: a case study of the Cheshmeh Khush Field, South Iran

Mahdi Rastegarnia[1], Ali Kadkhodaie-Ilkhchi[2]*
[1] *Petroleum Engineering Department, Faculty of Mining, Petroleum and Geophysics, Shahrood University of Technology, Shahrood, Iran*
[2] *Geology Department, Faculty of Natural Science, University of Tabriz, Tabriz, Iran*
**Corresponding author, e-mail: kadkhodaie_ali@tabrizu.ac.ir*
(*received: 27/06/2013 ; accepted: 26/11/2013*)

Abstract

Accurate permeability estimation has always been a concern in determining flow units, assigning appropriate capillary pressure and relative permeability curves to reservoir rock types, geological modeling, and dynamic simulation.Acoustic method can be used as an alternative and effective tool for permeability determination. In this study, a four-step approach is proposed for permeability estimation from acoustic data. The steps include estimation of the Stoneley wave slowness from conventional logs using a support vector machine neural network, determination of the Stoneley wave slowness in non-permeable zones, calculation of the Stoneley permeability index, and calculation of the Stoneley-Flow Zone Index (*ST-FZI*) permeability using the index matching factor (*IMF*). Finally, a comparison is made between the *ST-FZI* permeability with those derived from *CMR* log and core analysis. The results of this study show that acoustic method in conjunction with robust *SVM* neural network can be considered as an accurate tool for permeability estimation in the mixed clastic-carbonate reservoirs with complex pore type systems.

Keywords: *Cheshmeh Khush oilfield, Flow zone indicator, Permeability, Stoneley wave velocity, Well log data*

Introduction

Permeability estimation is a challenging issue in the carbonate reservoirs, and the factors affecting permeability are different from sandstone reservoirs. To date, many researchers have tried to obtain reservoir permeability from the Stoneley wave velocity (*DTST*). Rosenbaum (1974) was the first scholar to propose a method to predict permeability using the Stoneley wave. Williams *et al*. (1984) showed that deterministic correlations could be established between permeability and Stoneley attenuation. Theoretical models based on Biot's poroelastic theory have then been developed by Schmitt *et al*. (1988). Winkler *et al.,* (1989) combined laboratory measurements and petrophysical models based on Biot's theory and validated the acoustic based models. Tang *et al.,* (1991) proposed a simplified Biot-Rosenbaum model and developed a technique to invert the Stoneley wave amplitude to permeability. Cassell *et al.,* (1994) proposed a simple technique to extract the permeability indicator from the variations of the Stoneley attenuation. Tang *et al.,* (1996) described a fast algorithm to estimate the formation permeability using the Stoneley wave logs. They formulated a fast modeling technique to obtain the low-frequency Stoneley wave propagation in an irregular borehole (Tezuka *et al.,* 1997). Wu and Yin (2010) introduced a reliable method for determining reservoir permeability from the Stoneley wave attenuation, extracted from conventional sonic logs, by inversion of the full Biot wave equations for a porous medium.

Accurate permeability estimation has always been a problem in geological and petrophysical studies of hydrocarbon reservoirs. Nowadays, acoustic logging is faster and cheaper compared to the direct permeability determination methods, such as core measurement and well testing.

An alternative approach for permeability estimation is using well logging data as input predictors. However, due to scarcity of core samples, this alternative may not work in all cases. Accordingly, the Stoneley wave velocity measurements (if available) are logged for a continuous interval and provide many samples. Therefore, in the case of limited number of core samples, neural networks cannot provide satisfactorily estimations. DTST can fill this gap and if available can be considered as an alternative way for permeability estimation.

The present study uses the advantages of the Stoneley wave velocity in combination with other available conventional well logs and supports vector neural networks to estimate permeability in an instrumental way. The aims of the present research are as follows:

- *estimation of Stoneley wave slowness from conventional well logs,*
- *calculation of permeability index using DTST and FZI approaches,*
- *permeability estimation from the joint use of acoustic methods and SVR, and*
- *studying the correlation between Stoneley, CMR and core permeability.*

Study area

Data in this study came from three logged wells penetrated into the Asmari reservoir in the Cheshmeh Khush field (fig. 1); the core and log data are available for wells *A* & *B*. Data from well C comprise *CMR* log, Stoneley wave velocity, and log information for which core data are not present.

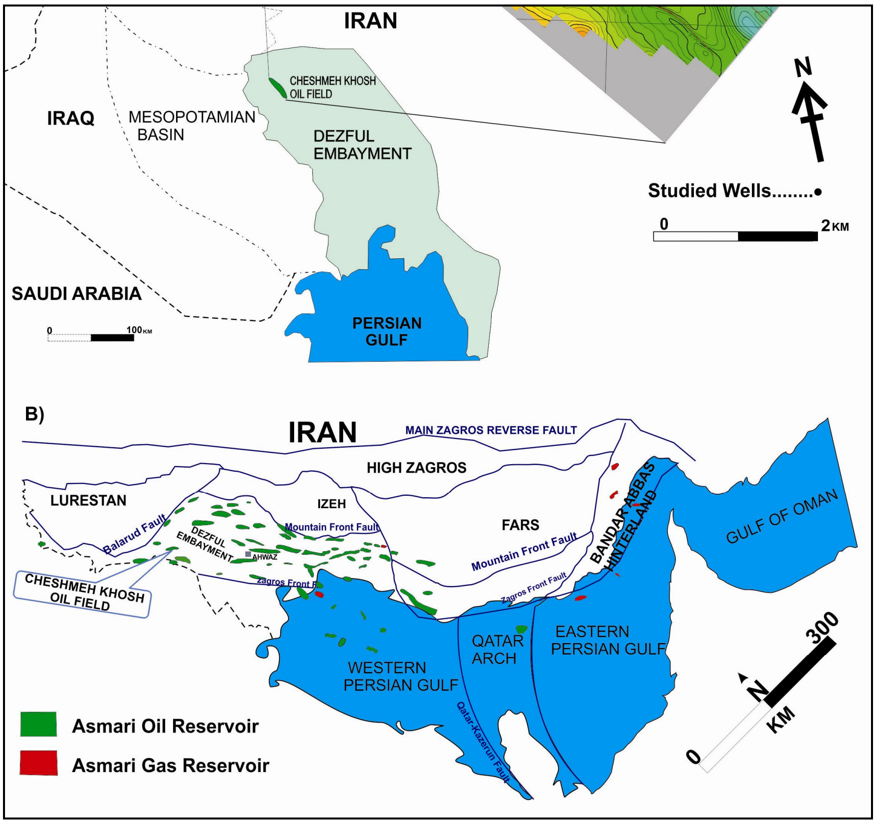

Figure 1: The location map of the Cheshmeh Khush oilfield in Dezful embayment

Support vector regression

Neural Networks (NNs) have been widely used and considered to be good non-linear regression methods for geosciences data estimation. However, the number of weights of the NNs is very high in cases with high dimensional input vectors (Han, D & Cluckie, I., 2004; Quang-Anh *et al.,* 2005; Liu, W.T *et al.,* 2006; Al-Anazi & Gates, 2010). Furthermore, these weights are optimized iteratively and this procedure is repeated with different initial settings, which might lead to non-global solutions. Recently, Support Vector Regression (SVR) emerged as an alternative regression tool. Simply, it is a derivation of Support Vector Machines (SVM), introduced by Vapnik (1995) (Lia, Q *et al.,* 2007; Bishop C. M., 2006). SVR acts as a specific type of learning algorithm characterized by the capacity control of the decision function, the use of the kernel functions (Table 1), and the sparsity of the solution.

It is a statistical method for creating regression functions of an arbitrary type from a set of training data (Wang, 2005; Hwei-Jen L. & Jih Pin Y, 2009).

In order to determine appropriate inputs for SVR model, the authors performed a stepwise regression by using forward selection and backward elimination. Forward selection involves starting with no variables in the model, testing the addition of each variable using a chosen model comparison criterion, adding the variable (if any) that improves the model the most, and repeating this process until none improves the model. Backward elimination involves starting with all of the candidate variables, testing the deletion of each variable using a chosen model comparison criterion, deleting the variable (if any) that improves the model the most, and repeating this process until no further improvement is possible. Application of the initial regression analysis showed that PHIE, DT, and RHOB log show the strongest relationship with the output (DTST).

Table 1: Polynomial, normalized polynomial, radial basis function (Gaussian) and Pearson universal (*PUK*) kernels (Wang, 2005)

Kernel Function	**Type of Classifier**
$K(x_i,x_j)=(x_i^{\mathrm{T}}x_j+1)^{\rho}$	Complete polynomial of degree ρ
$K(x_i,x_j)=\dfrac{(x_i^{\mathrm{T}}x_j+1)^{\rho}}{\sqrt{(x_i^{T}x_j)-(y_i^{T}y_j)}}$	Normalized polynomial kernel of degree ρ
$K(x_i,x_j)=\exp\left[\left\Vert x_i-x_j\right\Vert^2/2\sigma^2\right]$	Gaussian (Radial Basis Function) with parameters σ control the half-width of the curve fitting peak
$K(x_i,x_j)=\dfrac{1}{\left[1+\left(\dfrac{\left(2\sqrt{\left\Vert x_i-x_j\right\Vert^2}\sqrt{2^{1/\omega}-1}\right)}{\sigma}\right)^2\right]^{\omega}}$	Pearson VII Universal Kernel (PUK) with two parameters of σ and ω which control the Pearson width and the tailing factor of the curve fitting peak respectively

Normally, some justification can be made for physical relationships between the well log data used, Stoneley wave velocity, and permeability. Stoneley wave velocity (DTST) decreases as porosity and permeability increase. Accordingly, it is expected to see an inverse relationship between DTSE and formation permeability. Density log values show an inverse relationship with DTST due to an inverse relation between porosity and density. There is a direct relation between sonic log data (DT) and DTST, since they are from the same family.

In this study, SVR was employed as an intelligent model to formulate well log data to DTST. Then, through the synthesis of DTST, permeability was calculated for all wells comprising well log data.

Methodology

In the present study, a four-step approach is proposed for permeability estimation from acoustic data as follows:

a) estimation of the Stoneley wave slowness from conventional logs using a support vector machine neural network,

b) determination of the Stoneley wave slowness in non-permeable zones,

c) calculation of the Stoneley permeability index, and

d) calculation of the *ST-FZI* permeability by employing the index matching factor and Stoneley permeability index.

Finally, a comparison is made between the *ST-FZI* permeability with those derived from *CMR* log and core analysis.

Estimating stoneley wave slowness from well logs

In this section, a support vector regression model was designed to estimate the Stoneley wave slowness from conventional logs data in wells *A* & *B*. As mentioned earlier, the Stoneley wave slowness data were only available for well *C*. Therefore, the raw data of Asmari formation were initially clustered into sandstone and carbonate sets in the training well *C*. By using the stepwise regression method, the researchers selected the appropriate input variables to create a *SVR* model. They include sonic log (*DT*), density log (*RHOB*), and effective porosity data (*PHIE*). The input and output data were normalized in the range of 0 and 1. The optimal parameters of the SVR model (kernel and *C* value) for sandstone and carbonate intervals were achieved by trial and error (Table 2). The crossplot of the real and predicted Stoneley wave velocity in the testing samples is shown in fig. 2.

In the light of the acceptable results of the *SVR* model, *DTST* is estimated by using the conventional well log data in wells *A* and *B* (fig. 3).

Table 2: Optimal Kernel function and *C* values used in *SVR* model

Reservoir type	Kernel function	C	Regression model	R^2	SSE
Sandstone	Poly	50	0.955X+0.018	0.94	0.0027
Carbonate	Gaussian	3000	0.767X+0.054	0.85	0.0120

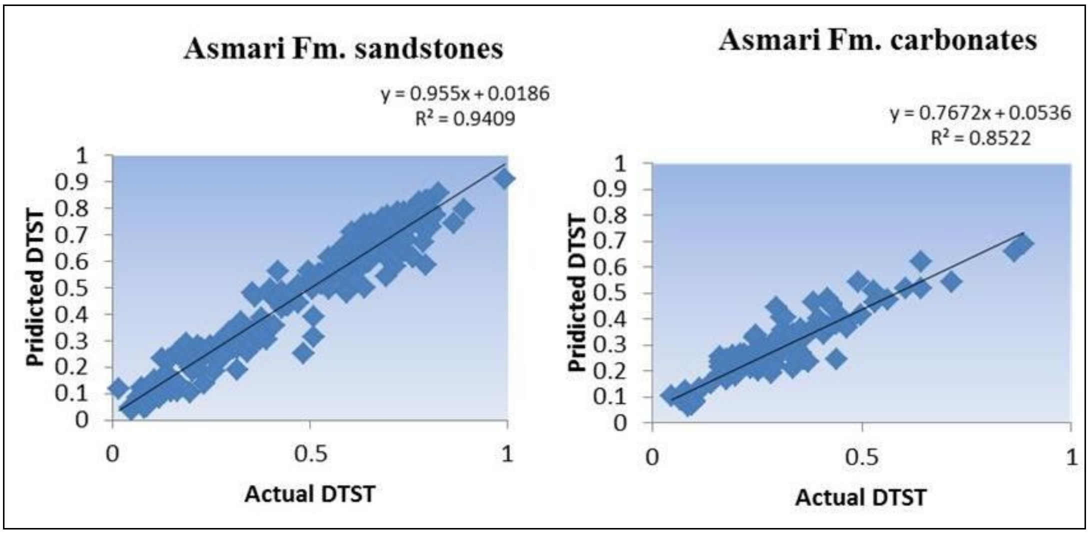

Figure 2: Crossplot showing a correlation coefficient between measured and estimated *DTST* from *SVR* model in carbonate and sandstone members of Asmari formation.

Calculating DTST in non-permeable zones (DTSTE)

To estimate permeability with this method we need some parameters such as Stoneley wave slowness, Stoneley wave slowness in non-permeable zones, volume of minerals (from formation evaluation results), and bulk density and index matching factor (*IMF*) for each mineral. Non-permeable zones include anhydrites, shales, and dense limestones.

The Stoneley wave slowness in non-permeable zones (*DTSTE*) can be calculated using two approaches (Winkler & Johnson, 1989):

a) Averaging the Stoneley wave slowness in non-permeable zones. This will result in *DTSTE*=245.38 μs/ft for non-permeable zones.

b) Crossplotting the Stoneley wave slowness versus effective porosity in the range of zero and 0.05. As shown in figure 4, the average value of *DTST* in dense limestones equals 243.17. Both methods produce close results; however, we prefer the second approach since it has a sound logic for identification of non-permeable zone (Winkler & Johnson, 1989).

Calculating stoneley permeability index (KIST)

KIST is calculated as the ratio of Stoneley slowness to Stoneley slowness in non-permeable zone as follows (Winkler & Johnson, 1989).

$$KIST = \frac{DTSE}{DTSTE} \qquad (1)$$

Where *KIST* is the Stoneley permeability index (fractional, range = 0 to 1), *DTST* is the Stoneley wave slowness of formation, and *DTSTE* is the Stoneley wave slowness in non-permeable zone. The Stoneley permeability index, *KIST*, is not an estimation of permeability, but it is an index of fluid movement in porous media around the borehole.

Calculating ST-FZI permeability

Since fluid movement is a function of pore throat distribution, pore shape, and pore size, the Stoneley permeability index is a tortuosity index only. These factors can be combined in a concept called Flow Zone Index (*FZI*).

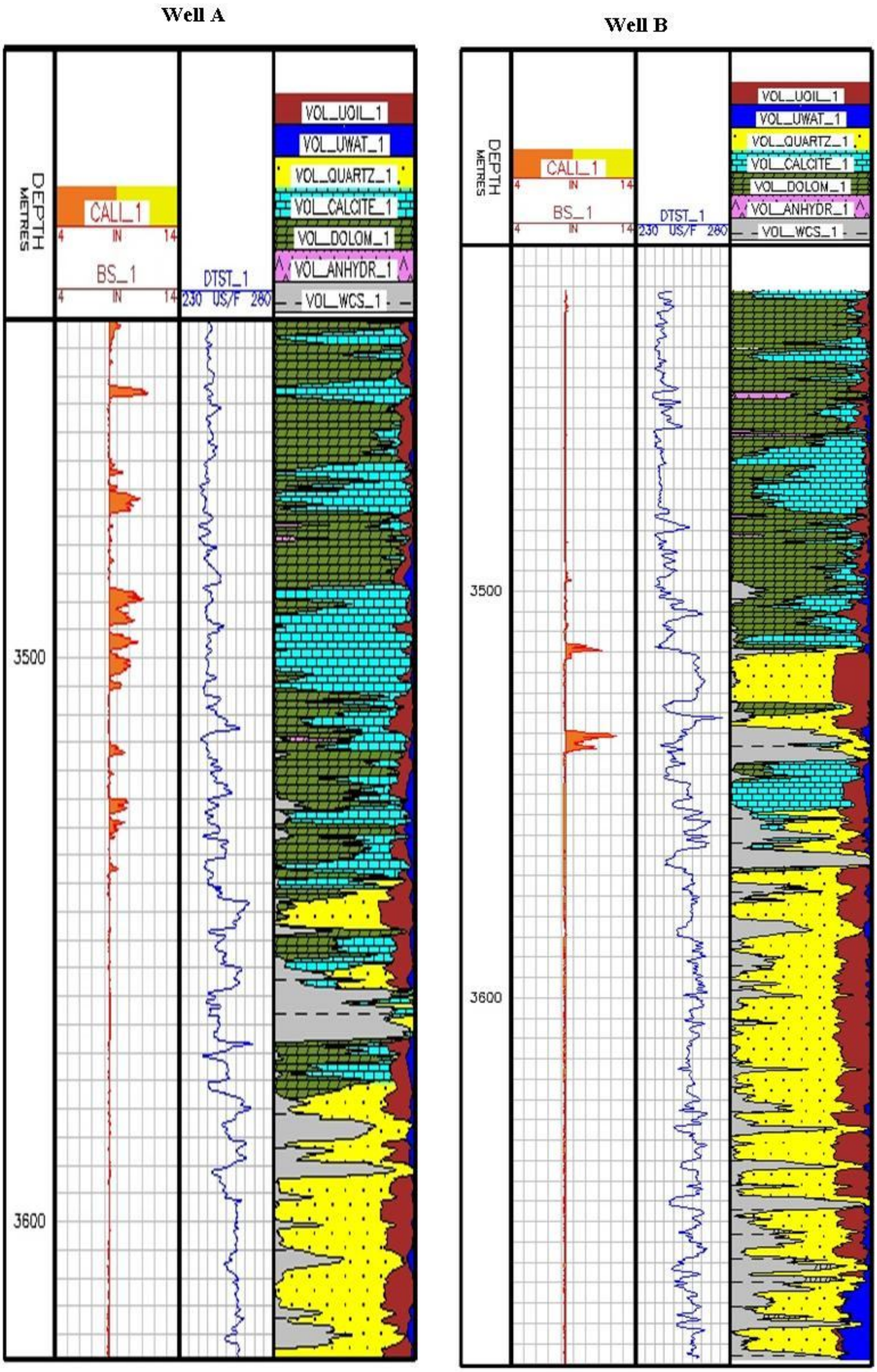

Figure 3: *DTST* derived from *SVR* model versus lithology column in wells *A* & *B*

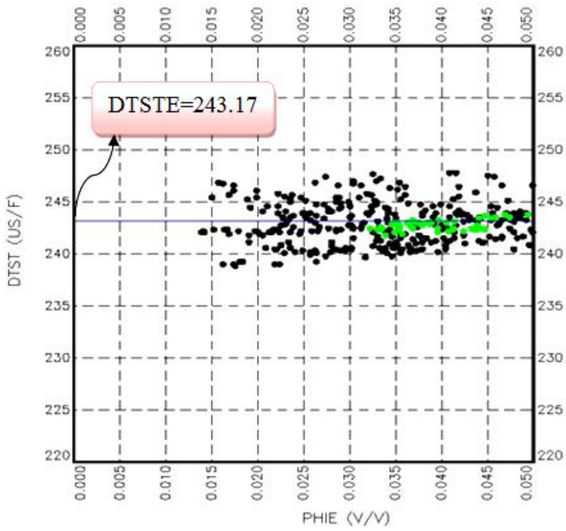

Figure 4: Crossplot of *DTST* versus effective porosity used to derive Stoneley wave slowness in non-permeable zone. Non-permeable zones are composed of anhydrite, shale and dense limestone. As *IMF* is zero for anhydrite and shale, *DTSTE* is calculated as high as 243.17 for dense limestones, points highlighted by green color.

The Stoneley permeability index is a direct measurement of *FZI*. Since *FZI* approaches zero when the Stoneley permeability index approaches 1 in non-permeable zones and both of them approach to infinity when permeability approaches infinity, then simple relationships can be derived between *FZI* and *KIST* as follows (Wu & Yin, 2010):

$$KIST \propto FZI \quad (2)$$

$$FZI \propto (KIST - 1) \quad (3)$$

To formulate *FZI* to *KIST* a constant called *IMF* is introduced to equation 4 as follows:

$$FZI = IMF(KIST - 1) \quad (4)$$

Where:

FZI = flow zone index

IMF = flow zone index matching factor

The index matching factor is calculated using equation 5 (Nabeed & Barati, 2003).

$$IMF = \sum_{i=1}^{n} IMF_i V_i \quad (5)$$

IMF is computed by summing the volume weighted *IMF* for each individual mineral in the model. Using equation 5, the researchers calculated the index matching factor for different depths so that the best match is achieved between the core permeability and permeability index. Since the permeability values are zero in shales and anhydrites, the index matching factor was set to zero in such non-permeable zones.

After conversion of *KIST* to *FZI, the* following equation was used to estimate $K_{ST\text{-}FZI}$ (Winkler & Johnson, 1989).

$$K_{ST-FZI} = 1014 * FZI^2 \left(\frac{\varphi^3}{1-\varphi^2}\right) \quad (6)$$

Cross-plots, showing the correlation coefficient between core and predicted permeability in Wells A and B, are shown in figure 5. Figures 6 and 7 show the permeability calculated from the *ST-FZI* method against the available information including core permeability, porosity, fluids, and lithology column.

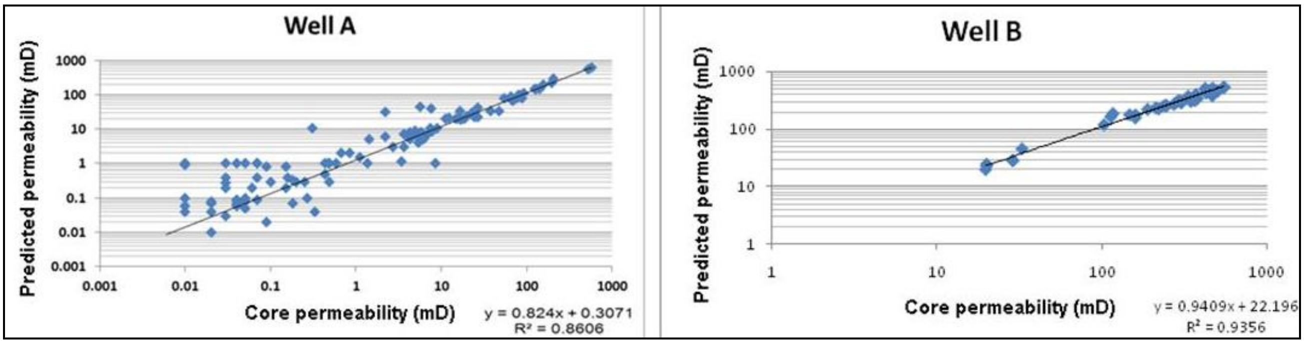

Figure 5: Cross-plots showing the correlation coefficient between core and predicted permeability in Wells A & B

Comparison of *ST-FZI* and core permeability

In this section, a comparison is made between the core permeability values and those estimated from the *ST-FZI* approach. Conventional core analysis (*CCAL*) data are available for the carbonate intervals of well *A* and sandstone intervals of well *B*. Graphical illustrations of figures 6 and 7 represent a comparison between the Stoneley (continuous red line) and core permeability (filled blue circles). Other rock properties including bore hole quality logs, porosity, reservoir electrofacies, and lithology column are also displayed. Hydraulic flow units (*HFUs*) were determined based on porosity and permeability data whose detailed specifications are given in Table 3. As is seen in Table 3, *HFUs* shown in red color have the highest reservoir quality with mean porosity and permeability of 0.189 p.u. and 203 mD, respectively. Flow units shown in gray, green, light blue and, dark blue colors receive the second to the fifth ranks from a reservoir quality point of view, respectively. As shown in figures 6 and 7, there is a good agreement between the results of acoustic method, core permeability, and hydraulic flow units (*HFUs*). Stoneley waves are most commonly generated during borehole sonic logging. They propagate along the walls of a fluid-filled borehole. They make up a large part of the low-frequency component of the signal from the seismic source and their attenuation is sensitive to fractures and formation permeability. Therefore, analysis of the Stoneley wave slowness is a useful approach to estimate formation permeability.

Table 3: Statistical parameters of hydraulic flow units (*HFUs*) derived from porosity and permeability data

Name	Color	Porosity	Permeability
HFU_5	Red	0.189	203
HFU_4	Gray	0.116	46.709
HFU_3	Green	0.076	0.900
HFU_2	Light blue	0.023	0.011
HFU_1	Dark blue	0.014	0.002

Comparison of *ST-FZI* CMR permeability

As mentioned earlier, *CMR* data are available for sandstone and carbonate intervals of well *C* from the studied field. In this section, we attempt to derive permeability from *CMR* log and make a comparison with the *ST-FZI* permeability.

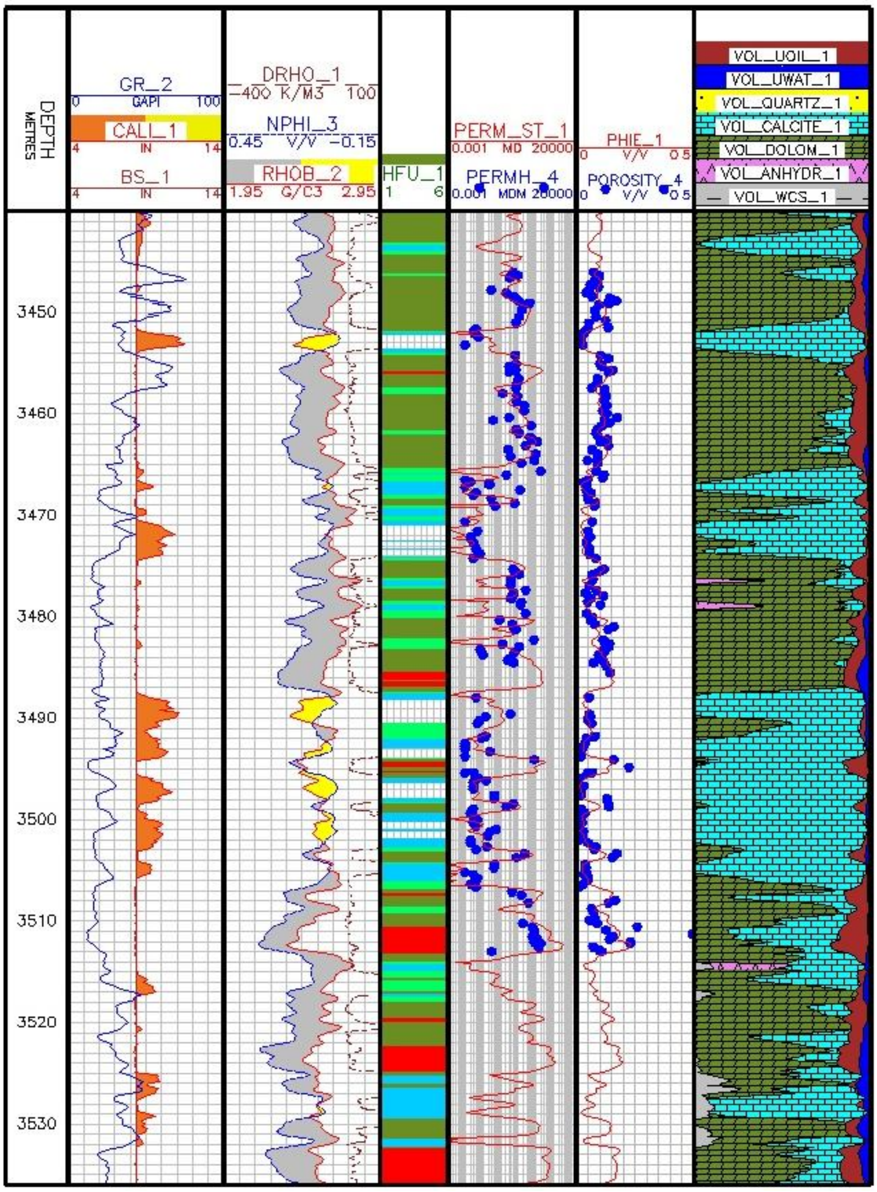

Figure 6: Graphical illustration of Stoneley permeability for carbonate interval in Well *A*

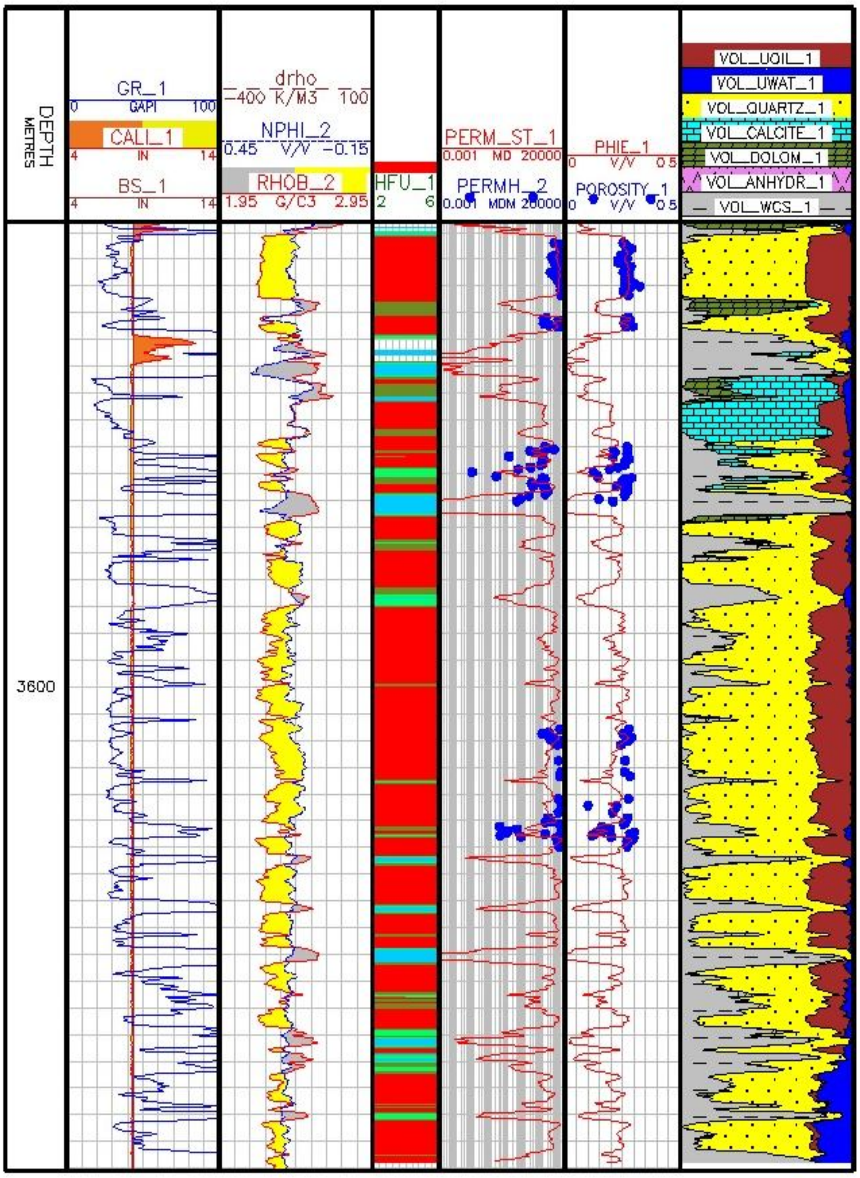

Figure 7: Graphical illustration of Stoneley permeability for sandstone interval in Well *B*

The Stoneley permeability of well *C* is estimated from equation 6 and a comparison is made with the permeability achieved from *CMR* log. The most important property of *CMR* measurement is the ability to record a continuous log of permeability. The Timur-Coates and Schlumberger Doll Research (*SDR*) equations were used to calculate formation permeability as follows.

a) The Timur-Coates equation

$$k_{Timur} = a.10^4.(\phi_{CMR})^4.\left(\frac{FFI}{BVI}\right)^2 \tag{7}$$

where the constant a equals 1mD, Bound Volume Index $(BVI) = \phi.Swir$ and Free Fluid Index $(FFI) = \phi.(1 - Swir)$

b) The SDR equation

The *SDR* equation was used as an alternative method for permeability estimation as follows.

$$k_{SDR} = C.(\phi_{CMR})^4.(T_{2\log})^2 \tag{8}$$

where the constant C equals 4 for sandstones and 0.1 for carbonates. Both equations are highly dependent on porosity.

The cross-correlation of *CMR* and *ST-FZI* permeability for the sandstone and carbonate intervals of well *C* are displayed in Tables 4 and 5. There is a good agreement between the Stoneley wave slowness and *CMR* permeability in sandstone intervals. However, the correlation becomes weak in carbonate members.

Table 4: Cross-correlation of *CMR* and *ST-FZI* permeability for sandstone intervals of well *C*

Sandstones (R^2)	**K_{SDR}**	**K_{timur}**	**.Perm-ST**
K_{SDR}	1	94.77%	73.21%
K_{timur}		1	79.89%
Perm-ST			1

Table 5: Cross-correlation of *CMR* and *ST-FZI* permeability for carbonate intervals of well *C*

Carbonate (R^2)	**K_{SDR}**	**K_{Timur}**	**.Perm-ST**
K_{SDR}	1	90%	36.66%
K_{Timur}		1	39.17%
Perm-ST			1

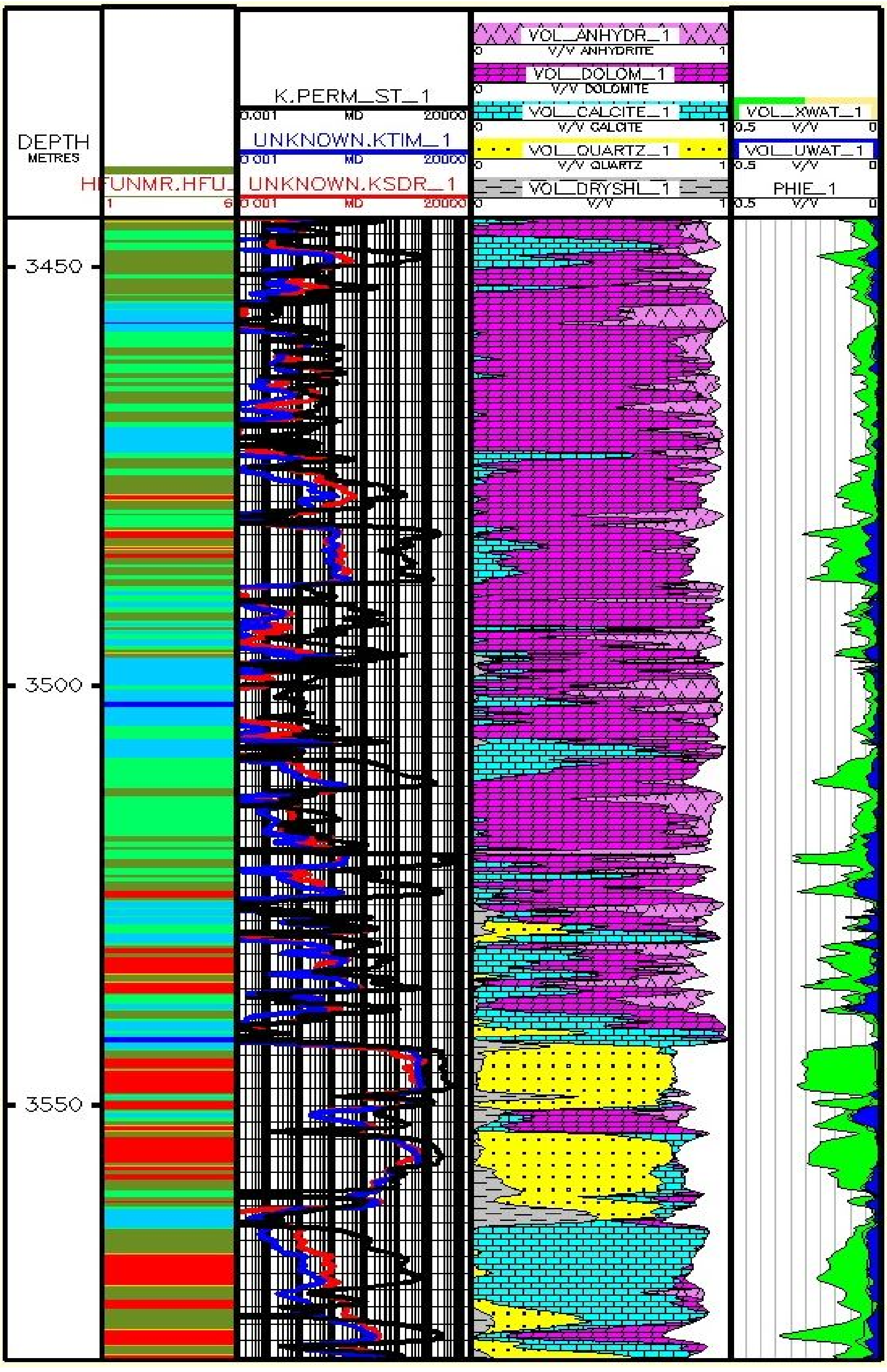

Figure 8: Comparison of *CMR* and *ST-FZI* permeability for mixed carbonate/sandstone intervals in well *C*

This mismatch is attributed to the uncertainty in determination of *T2* distribution cut-off to separate free fluids from bound fluids. Normally, *T2* cutoff value is considered as 92 ms for carbonate rocks. However, this value could vary from 90 ms to 700 ms due to reasons such as lithology heterogeneity, complex pore type system, and presence of isolated secondary porosities like moldic and vuggy in carbonate reservoirs.

In both carbonate and sandstone reservoirs, the correlation between K_{Timur} and *ST-FZI* permeability is higher than K_{SDR}. This could be attributed to the following reasons:

a) Changes in *T2* distribution which affect T_{2LM} are not considered in K_{Timur} while being considered for K_{SDR}.

b) Irrespective of K_{SDR}, the Timur-Coates permeability is not affected by formation fluid type. Change in fluid type will cause a change in *T2* distribution curve and consequently a change in T_{2LM}, whereas *BVI* and *BVM* values will remain unchanged.

It can be stated that Stoneley wave velocity data are good indicators of permeability. As they are not available for all wells we used SVR neural networks to simulate them from well logs. As can be seen in Table 5 and graphical illustrations of figure 6 & 7 comparing KSDR, KTimur, KSTN with core permeability direct using of well logs cannot perform as accurate as Stoneley data. So, it is not recommended to directly use well log data for permeability estimation when Stoneley data are available.

A comparison of *CMR* and *ST-FZI* permeability in the mixed carbonate/sandstone intervals of well *C* is illustrated in figure 8. Unfortunately, there is no measured core porosity and permeability data for well *C* to assess the reliability of the acoustic and *CMR* methods. Nontheless, it could be claimed that *CMR* logging and acoustic methods have different concepts and physics of measurement, but they reach close results for permeability estimation. This could be a confirmation of permeability estimated from acoustic methods used in this study.

Conclusion

In the present study, a four-step approach is proposed to estimate permeability by using support vector machines and acoustic methods. Unfortunately, there is no simple equation to calculate permeability from the Stoneley wave slowness. The results of this research revealed that calibration of the Stoneley wave slowness log, with core data in the framework of the hydraulic flow units approach, provides high accuracy estimations of reservoir permeability.

The Timur-Coates and *SDR* equations, which were used to derive permeability from *CMR* log, were not successful in carbonate intervals. This mismatch is attributed to the high sensitivity of $T_{2cutoff}$ to pore types in carbonate rocks. Unlike sandstones in which petrophysical properties are highly dependent on porosity, there is no such a simple relationship in carbonate rocks due to their complex mineralogy and pore types system. For this reason, pore types classification and calibration of $T_{2cutoff}$ values with capillary pressure data are expected to give better results in calculating permeability.

Parameter setting and training of the *SVR* networks are easier and faster in comparison to the conventional neural networks such as *MLP*, *RBF,* and *PNN*. It performs well in data transmission to the higher dimensions and non-linear systems.

Acknowledgments

We would like to offer our sincere gratitude to the Iranian Central Oilfields Company (*ICOFC*) for their financial support, constructive cooperation, and providing us with the necessary data throughout the project.

References

Al-Anazi, A., Gates, I.D. 2010. Capability of Support Vector Machines to Classify Lithology from Well Logs in heterogeneous reservoirs. Engineering Geology, 114: 267-277.

Bishop C.M., 2006. *Pattern Recognition and Machine Learning*, Springer, Berlin, Heidelberg.

Cassell, B., Badri, M., Faulhaber, J. 1994. Permeability Prediction Based on Anelastic Attenuation Using Dipole Shear and Low Frequency Monopole Sources in a Carbonate Reservoir in Saudi Arabia. *GEO-94 Middle East Geosciences Exhibition & Conference*, Bahrain, April 25-27.

Han, D., Cluckie, I. 2004. Support vector machines identification for runoff modeling. In "Liong S.Y., Phoon K.K., Babovic V. (Eds.). *Proceedings of the Sixth International Conference on Hydroinformatics*, Singapore, June 21-24.

Hwei-Jen, L., Jih Pin, Y. 2009. Optimal reduction of solutions for support vector machines. Applied Mathematics and Computation 214, 329-335.

Lia, Q., Licheng, J., Yingjuan, H. 2007. Adaptive simplification of solution for support vector machine. *Pattern Recognition* 40, 972-980.

Liu, W.T., Xie X., Tang, W., Zlotnicki, V. 2006. Space based observations of oceanic influence on the annual variation of South American water balance. Geophysical. Research Letters 33, L08710. doi: 10.1029/2006GL02568

Nabeed, A.A, Barati A. 2003. New Hydraulic Unit Permeability Approach with DSI. *SPWLA 9th Formation Evaluation Symposium*, Japan, September, 25-26.

Quang-Anh, T., Xing, L., Haixin, D. 2005. Efficient performance estimate for one-class support vector machine. Pattern Recognition Letters 26, 1174–1182.

Rosenbaum, J.H. 1974. Synthetic microseismograms logging in a porous formation, Journal of Geophysics 39, 1-32.

Schmitt, D.P. Bouchon, M. Bonnet, G. 1988. Full-wave Synthetic Acoustic Logs in Radially Semi-infinite Saturated Porous Media. Journal of Geophysics, 53: 807-823.

Tang, X.M., Cheng, C.H., Toksoz, M.N. 1991. Dynamic Permeability and Borehole Stoneley Waves: A Simplified Biot-Rosenbaum Model. Journal of the Acoustical Society of America 90: 1632-1646.

Tezuka, K., Cheng, C.H., Tang, X.M. 1997. Modeling of low-frequency Stoneley-wave propagation in an irregular borehole, Geophysics, 62: 1047-1058.

Vapnik, V. 1995, The Nature of Statistical Learning Theory. New York: Springer, USA.

Wang, L. 2005. Support Vector Machines: Theory and Applications, Nanyang Technological University, School of Electrical & Electronic Engineering, Springer, Berlin, Heidelberg.

Williams, D.M., Zemanek, J., Angona, F.A., Dennis, C.L., Caldwell, R. L. 1984. The long spaced acoustic logging tool, *The 25th Annual Logging Symposium*, New Orleans, LA, June 10-13.

Winkler, K.W., Liu, H.L., Johnson, D.L. 1989. Permeability and borehole Stoneley waves: comparison between experiment and theory. Journal of Geophysics, 54: 66-75.

Wu, X., Yin, H. 2010. Method for determining reservoir permeability form borehole Stoneley-wave attenuation using Biot's poroelastic theory, US patents. USPC Class: 16625002, Patent application number: 20090145600.